



## Mitochondrial pyruvate carrier in *Trypanosoma brucei*.

Jitka Štáfková, Jan Mach, Marc Biran, Zdeněk Verner, Frédéric Bringaud, Jan Tachezy

### ► To cite this version:

Jitka Štáfková, Jan Mach, Marc Biran, Zdeněk Verner, Frédéric Bringaud, et al.. Mitochondrial pyruvate carrier in *Trypanosoma brucei*.. *Molecular Microbiology*, 2016, 100 (3), pp.442-56. 10.1111/mmi.13325 . hal-02404835

**HAL Id: hal-02404835**

**<https://cnrs.hal.science/hal-02404835>**

Submitted on 3 Nov 2023

**HAL** is a multi-disciplinary open access archive for the deposit and dissemination of scientific research documents, whether they are published or not. The documents may come from teaching and research institutions in France or abroad, or from public or private research centers.

L'archive ouverte pluridisciplinaire **HAL**, est destinée au dépôt et à la diffusion de documents scientifiques de niveau recherche, publiés ou non, émanant des établissements d'enseignement et de recherche français ou étrangers, des laboratoires publics ou privés.

# Mitochondrial pyruvate carrier in *Trypanosoma brucei*

AQ7 4 Jitka Štáfková,<sup>1</sup> Jan Mach,<sup>1</sup> Marc Biran,<sup>2</sup>  
3 Zdeněk Verner,<sup>1</sup> Frédéric Bringaud<sup>2,3</sup> and  
6 Jan Tachezy<sup>1\*</sup>  
7 <sup>1</sup>Department of Parasitology, Faculty of Science,  
8 Charles University in Prague, Czech Republic.  
9 <sup>2</sup>Centre de Résonance Magnétique des Systèmes  
10 Biologiques (RMSB) and <sup>3</sup>Laboratoire de  
11 Microbiologie Fondamentale et Pathogénicité (MFP),  
12 UMR5234 CNRS, Université de Bordeaux, Bordeaux,  
AQ2 13 France

## Summary

Pyruvate is a key product of glycolysis that regulates the energy metabolism of cells. In *Trypanosoma brucei*, the causative agent of sleeping sickness, the fate of pyruvate varies dramatically during the parasite life cycle. In bloodstream forms, pyruvate is mainly excreted, whereas in tsetse fly forms, pyruvate is metabolized in mitochondria yielding additional ATP molecules. The character of the molecular machinery that mediates pyruvate transport across mitochondrial membrane was elusive until the recent discovery of mitochondrial pyruvate carrier (MPC) in yeast and mammals. Here, we characterized pyruvate import into mitochondrion of *T. brucei*. We identified *mpc1* and *mpc2* homologs in the *T. brucei* genome with attributes of MPC protein family and we demonstrated that both proteins are present in the mitochondrial membrane of the parasite. Investigations of *mpc1* or *mpc2* gene knock-out cells proved that *T. brucei* MPC1/2 proteins facilitate mitochondrial pyruvate transport. Interestingly, MPC is expressed not only in procyclic trypanosomes with fully activated mitochondria but also in bloodstream trypanosomes in which most of pyruvate is excreted. Moreover, MPC appears to be essential for bloodstream forms, supporting the recently emerging picture that the functions of mitochondria in bloodstream forms are more diverse than it was originally thought.

## Introduction

Pyruvate is a central intermediate metabolite involved in many cellular catabolic and anabolic pathways. This compound is the cytosolic product of glycolysis, and in most eukaryotic cell types, pyruvate enters the mitochondria for further oxidation to acetyl-CoA to fuel the tricarboxylic acid cycle. Thus, pyruvate represents an important branching point in cellular metabolism for balancing glycolysis and oxidative phosphorylation.

The availability of pyruvate in the mitochondrion is determined through a specific carrier located in the inner mitochondrial membrane. The principal biochemical features of mitochondrial pyruvate carrier (MPC) were characterized in the 1970s. Pyruvate is symported with one proton, and this transport is driven by  $\Delta pH$  (Papa *et al.*, 1971; Halestrap, 1978). However, the molecular identity of MPC has only recently been revealed, and currently MPCs have been characterized in *Saccharomyces cerevisiae*, *Drosophila melanogaster*, *Homo sapiens* (Bricker *et al.*, 2012; Herzig *et al.*, 2012) and *Arabidopsis thaliana* (Li *et al.*, 2014).

The mitochondrial pyruvate carrier comprises two small hydrophobic paralogous proteins, MPC1 and MPC2, which are essential and sufficient for the transport of pyruvate into mitochondria (Bricker *et al.*, 2012; Herzig *et al.*, 2012). In *S. cerevisiae*, a third paralog, MPC3, exists, sharing 71% amino acid sequence identity with MPC2, and MPC3 expression is induced upon growth on nonfermentable carbon sources (Herzig *et al.*, 2012; Timon-Gomez *et al.*, 2013; Bender *et al.*, 2015).

Structural predictions have revealed 2-3 transmembrane (TM) helices in all MPC homologs (Bricker *et al.*, 2012; Herzig *et al.*, 2012). Pfam lists MPC proteins as members of the MtN3-like clan, together with SWEET transporters ('Sugars Will Eventually be Exported Transporters') and the PQ-loop protein family (Finn *et al.*, 2014). A previous study suggested that the structure of prokaryotic SemiSWEET transporters, members of the same diverse clan, is similar to that of MPC (Vanderperre *et al.*, 2014).

*Trypanosoma brucei* is a pathogen of livestock and humans transmitted through tsetse flies in sub-Saharan Africa. The different life-cycle stages of trypanosomes present specific adaptations to their environments. For the bloodstream (BSF) and procyclic (PCF) forms of

*T. brucei*, these adaptations include changes in mitochondrial morphology, function, and overall metabolic rearrangements reflected by different spectra of metabolic end products. In BSF, ATP is primarily generated through glycolysis, and pyruvate is the predominant excreted end product of metabolism (Creek *et al.*, 2015). In contrast, PCF that live in the midgut of the insect vector where nutrients are scarce, depend on the mitochondrial catabolic pathway for ATP production. Pyruvate is utilized for substrate level phosphorylation, resulting in the production of acetate and ATP. In addition, proline and threonine are important carbon sources for these stages when glucose is limited. In glucose-depleted media, proline is metabolized to alanine, glutamate, CO<sub>2</sub> and succinate, whereas the end products of threonine metabolism are acetate and glycine (Linstead *et al.*, 1977; Lamour *et al.*, 2005).

The regulation of pyruvate availability in the mitochondrion is one of the mechanisms for balancing oxidative phosphorylation and glycolysis (Vanderperre *et al.*, 2014; Bender *et al.*, 2015). Similarly to yeast grown on fermentable carbon substrates, in BSF *T. brucei*, this balance is predominantly shifted towards glycolysis. Recently, a plasma membrane pyruvate transporter has been characterized in *T. brucei* (Sanchez, 2013); however, there is no information regarding the molecular characteristics of pyruvate transporters in mitochondria. Therefore, the aim of the present study was to determine whether *T. brucei* transports pyruvate into the mitochondrion using a putative MPC homolog and address the relative importance of pyruvate and the pyruvate transporter in PCF and BSF trypanosomes.

## Results

### MPC homologs in *T. brucei*

Two genes encoding putative MPC proteins were identified in the *T. brucei* genomic database ([www.tritrypdb.org](http://www.tritrypdb.org)) after a BLAST search of MPC1, MPC2 and MPC3 from *S. cerevisiae*: Tb927.9.3780, annotated as 'hypothetical protein, conserved' was the only result for the ScMPC1 query, while Tb927.7.3520, annotated as 'mitochondrial pyruvate carrier protein 2, putative', resulted from BLAST searches using both ScMPC2 and ScMPC3 as queries. Multiple protein alignment was generated using homologs from different organisms and edited by BMGE (Supporting Information Fig. S1), and an unrooted phylogenetic tree F1 was reconstructed using PhyML and MrBayes (Fig. 1A).

The tree shows that Tb927.9.3780 and Tb927.7.3520 clustered with MPC1 and MPC2/3 orthologs, respectively, with high statistical support. Based on this analysis, the corresponding *T. brucei* proteins were designated as TbMPC1 and TbMPC2. Subsequently, a series of *in silico* analyses

was performed. The results from MitoProt II and PSORTII, which predict mitochondrial targeting sequences and sub-cellular protein locations, indicated the mitochondrial localization of both TbMPC1 and TbMPC2 (the calculated probability of mitochondrial import was 0.85 and 0.83, respectively, according to MitoProt II; the PSORTII k-NN prediction was 47.8% mitochondrial for TbMPC1 and 43.5% cytosolic for TbMPC2). TMpred and TMHMM were used to predict the location of putative transmembrane helices in TbMPCs and all eukaryotic MPC homologs described thus far (Fig. 1B). Experimental evidence for the membrane topology of ScMPC1 and ScMPC2 according to Bender *et al.* (2015) was considered. Similar to other analyzed MPCs, TbMPC1 and TbMPC2 contain two and three transmembrane domains, respectively. Notably, in all MPC sequences, a tryptophan residue is conserved in the putative binding pocket in MPC2 (W89 in TbMPC2), and this amino acid position is substituted with phenylalanine, another aromatic amino acid, in MPC1 (F52 in TbMPC1). The proline forming the hinge region of the SemiSWEET transporter is conserved in all selected MPC2 and most MPC1 homologs, while trypanosomatid MPC1 revealed a proline-alanine substitution (P50 in TbMPC2, A15 in TbMPC1; Fig. 1B).

Based on the results from the *in silico* analysis, we concluded that the predicted *T. brucei* MPCs are evolutionary and structurally related to known MPC proteins.

### TbMPC1 and TbMPC2 localization

To determine the cellular localization of MPC paralogs in the PCF and BSF *T. brucei*, we prepared constructs for expression of TbMPC1 and TbMPC2 with a C-terminal epitope tag. We established PCF cell lines expressing both epitope-tagged TbMPC1 and TbMPC2 and an epitope-tagged TbMPC1 BSF cell line. Despite multiple attempts, we were not successful in obtaining a BSF cell line expressing epitope-tagged TbMPC2.

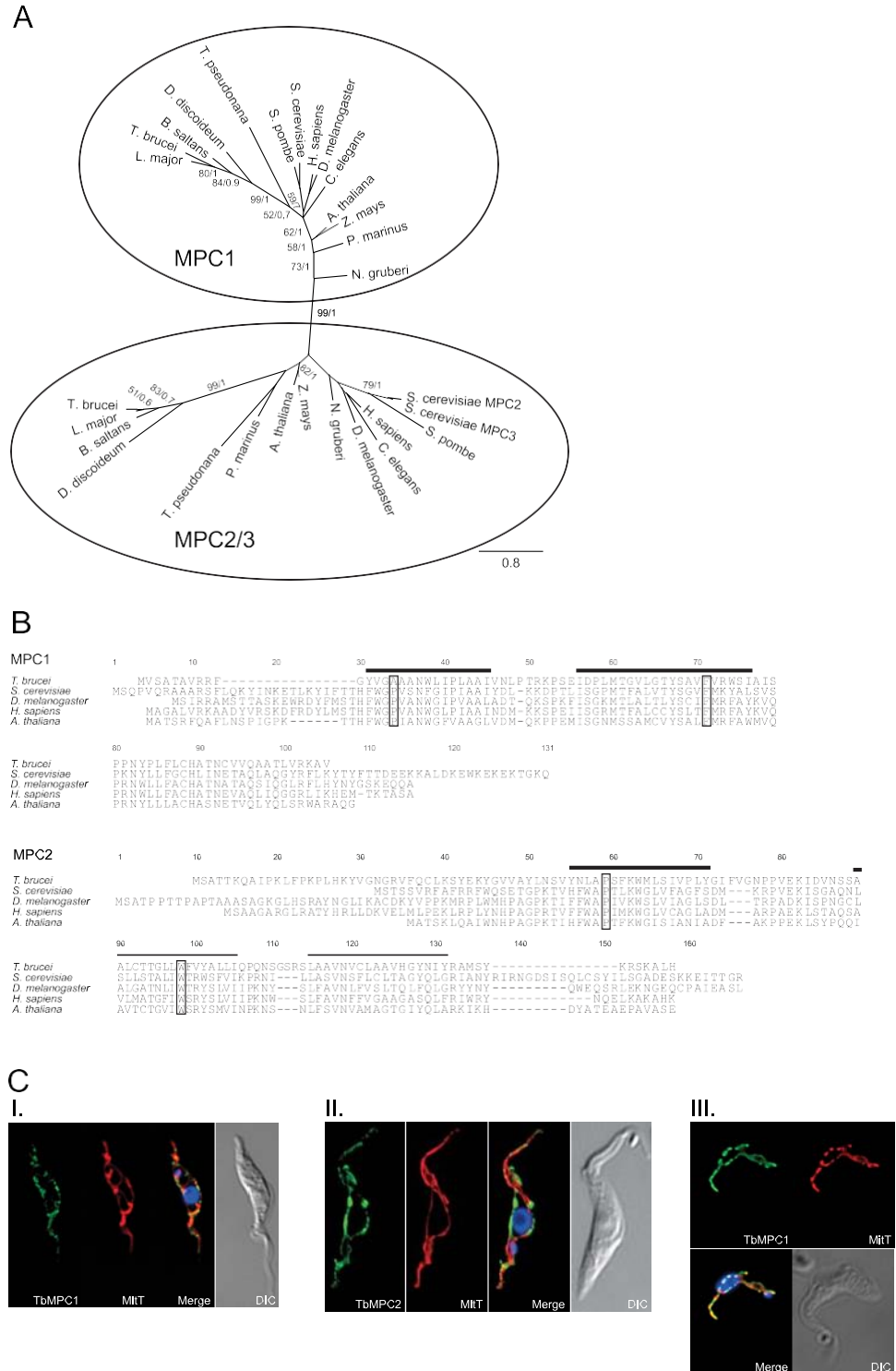
The localization of TbMPC1 and TbMPC2 was investigated using immunofluorescence microscopy and Western blotting of subcellular fractions (Fig. 1C, Supporting Information Fig. S2). In PCF, both TbMPC1 and TbMPC2 were observed in reticular structures that colocalized with mitochondrial MitoTracker staining (Fig. 1C, panels I, II). To prove the presence of TbMPCs in the mitochondrial membrane, we fractionated crude mitochondrial preparations to obtain mitochondrial matrix-enriched and membrane-enriched fractions. Western blot analysis confirmed the presence of both TbMPC1 and TbMPC2 only in the membrane fractions (Supporting Information Fig. S2). Mitochondrial membrane localization of TbMPC1 was demonstrated also in BSF (Fig. 1C, panel III and Supporting Information Fig. S2).

**Fig. 1.** Phylogeny and localization of MPC1 and MPC2/3.

**A.** An unrooted phylogenetic tree was reconstructed using 29 selected known and predicted MPC homologs. The sequences branched into two distinct clades containing MPC1 or MPC2. Bootstrap values higher than 50 are shown together with posterior probability. The scale bar shows the number of substitutions per site. The sequence alignment, full species names and accession numbers are shown in Supporting Information Fig. S1.

**B.** Alignments of *T. brucei* MPC1 and MPC2 protein sequences to corresponding orthologs with experimentally confirmed function. Common predicted transmembrane domains (TMpred) are highlighted by a black line. Boxed amino acids correspond to the selected conserved amino acid residues present in functionally important regions of SemiSWEET transporter [substrate-binding pocket and the PQ 'hinge' region aiding the binder clip-like motion of the transporter (Lee *et al.*, 2015)].

**C.** Immunofluorescent visualization of *T. brucei* MPC in PCF (I, II) and BSF (III) cells. Antibodies against V5 and HA tags were used to detect TbMPC1 and TbMPC2 (green) in PCF, respectively. V5-tagged TbMPC1 was detected in BSF. MitoTracker (MitT) was used to visualize mitochondria (red), and DAPI was used to visualize nuclei and kinetoplasts (blue). DIC, differential interference contrast.



191 *Generation of TbMPC1 and TbMPC2 PCF null mutants*  
 192 *and pyruvate uptake analysis*

193 Deletion of the *tbmcp1* or *tbmcp2* gene was accomplished  
 194 in wild type PCF (strain 427) by two rounds of transforma-  
 195 tion in which the ORFs were replaced by an antibiotic

resistance gene. Deletion of both alleles was confirmed in 196  
 several clones by PCR, and clones B6 (*Dtbmpc1*-B6) and 197  
 2C4 (*Dtbmpc2*-2C4) were selected for further experiments 198  
 (Fig. 2A). Growth of both KO clones in glucose-containing 199 F2  
 SDM-79 was not significantly affected (Fig. 2B). Thus, 200

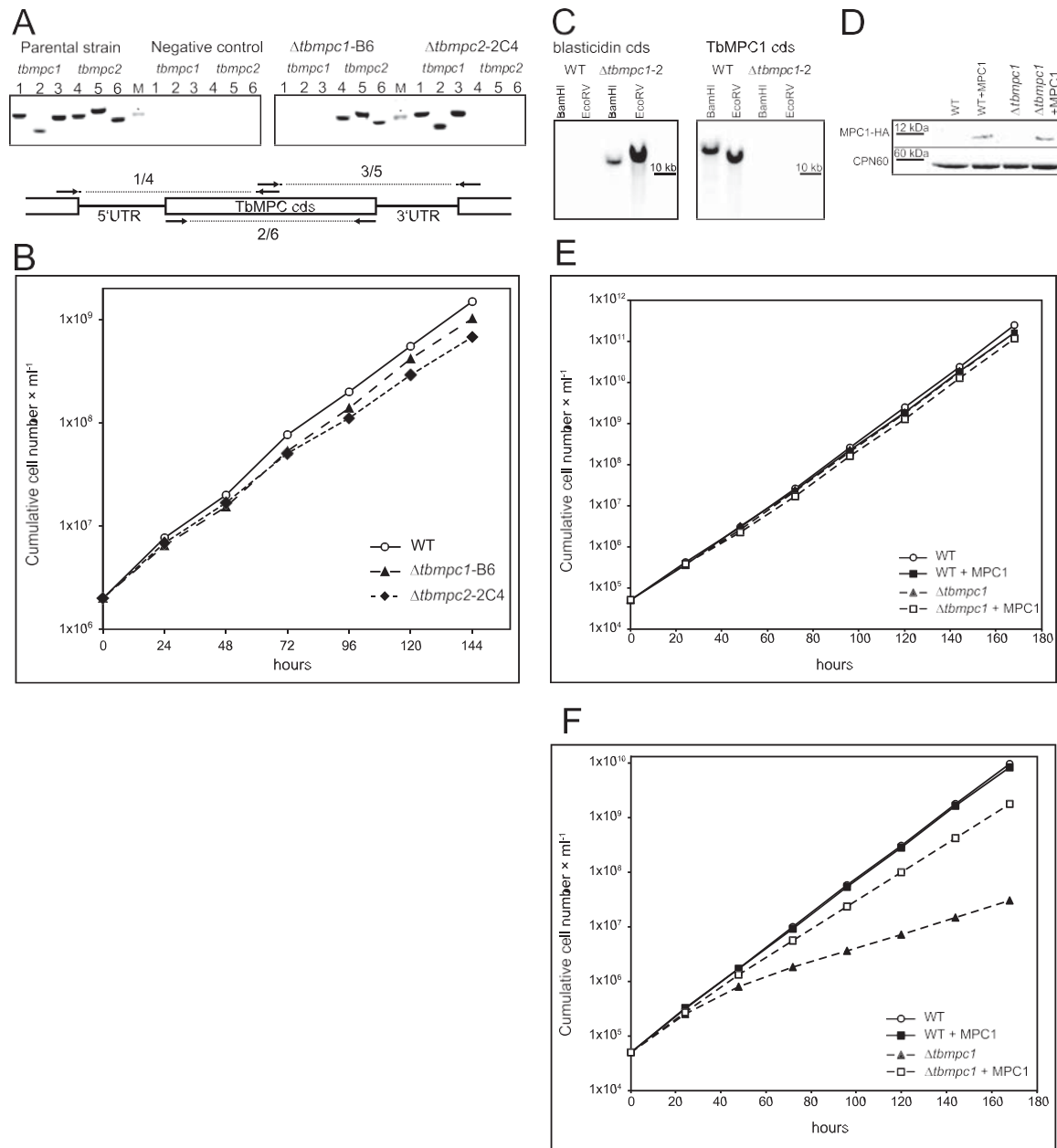


**Fig. 2.** Analysis of the genotype and growth phenotype of *Dtbmpc1*-B6 and *Dtbmpc2*-2C4 in PCF cell lines, and *Dtbmpc1*-2 and knock-in cell lines expressing *TbMPC1*-HA in BSF.

**A.** PCR analysis of genomic regions flanking *tbmpc*-coding sequences in wild type and null mutant cell lines. Primers in the *mpc* coding region and external to the cassette insertion were used (scheme and Supporting Information Table S1). Water instead of DNA was used in the negative control. M: molecular weight marker (\*, 500 bp).

**B.** *In vitro* growth of the wild type PCF strain (open circles), *Dtbmpc1*-B6 (triangles) and *Dtbmpc2*-2C4 (diamonds) cell lines. Average values of three independent experiments are shown; relative standard deviation was consistently below 10%.

**C.** Verification of the *tbmpc1* deletion in the selected *Dtbmpc1* clone 2 using Southern blot analysis. The membranes were probed against *TbMPC1* and blasticidin deaminase coding regions.

**D.** Expression of *TbMPC1*-HA determined by Western blotting in wild type, *Dtbmpc1*-2, and knock-in BSF cell lines in wild type and *Dtbmpc1*-2 background. HSP60 expression was visualized as loading control.

**E, F.** Growth of BSF wild type (circles), *Dtbmpc1*-2 (triangles) and knock-in cell lines (wild type 1 *TbMPC1*-HA, full squares; *Dtbmpc1*-2 1 *TbMPC1*-HA, open squares) in HMI-9 (E) or CMM (F). Average values of three independent experiments are shown; relative standard deviation was consistently below 10%.



AQ1

neither TbMPC1 nor TbMPC2 is essential under standard culture conditions.

The role of TbMPC1 and TbMPC2 in pyruvate import to mitochondria of PCF trypanosomes was assessed by measurement of  $^{14}\text{C}$ -pyruvate uptake by mitochondrial fractions of wild type cells and respective null mutants (*Δtbmpc1*-B6, *Δtbmpc2*-2C4). Incorporation of radioactivity in mitochondrial preparations from both mutant cell lines was decreased by approximately 60% compared with wild type samples. A similar decrease in pyruvate uptake was observed in wild type mitochondria incubated with UK-5099, an inhibitor of MPC and monocarboxylate transporters (Halestrap, 1975). On the contrary, UK-5099 did not affect pyruvate uptake by mitochondrial preparations from either mutant cell line (Fig. 3). These results indicate that both TbMPC1 and TbMPC2 are needed for inhibitor-sensitive pyruvate import into mitochondria and confirm that MPC-mediated pyruvate uptake in the mitochondrion is abolished in both mutant cell lines.

#### Analysis of metabolic end products in *Δtbmpc1*-B6 and *Δtbmpc2*-2C4 PCF cell lines

In PCF trypanosomes, phosphoenol pyruvate derived from glycolysis is further metabolized to succinate in the glycosome, or in the form of pyruvate, it enters mitochondria, where it is metabolized to acetate and succinate (Fig. 4). Therefore, we investigated the effect of *tbmpc1*

and *tbmpc2* gene knockouts on the glucose-dependent formation of metabolic end products. In PCF, pyruvate production was increased in both *Δtbmpc1*-B6 and *Δtbmpc2*-2C4 cell lines compared with wild type samples, consistent with defective pyruvate transport into the mitochondrion. In addition, a significant decrease in acetate and succinate production was observed in these mutant cell lines (Table 1). Reduced acetate generation in the T1 mitochondrion is consistent with a reduction in mitochondrial pyruvate metabolism. Null mutants also displayed a

trend towards diminished lactate production ( $P = 0.07$ ). It should be noted that pyruvate cannot be reduced to lactate in *T. brucei* due to the lack of lactate dehydrogenase activity. Lactate detected in our assays is expected to be a product of detoxification of methylglyoxal which arises spontaneously in the course of glycolysis (Greig *et al.*, 2009). Changes in pyruvate, acetate, succinate and lactate levels in wild type samples incubated with UK-5099 showed patterns similar to those observed in mutant cell lines, albeit these effects were less pronounced. As expected, the presence of the inhibitor did not affect acetate, succinate and lactate levels in mutant cell lines. Together, these results provide further evidence for the involvement of TbMPC1 and TbMPC2 in mitochondrial pyruvate transport.

To confirm these data, the end products of glucose and/or threonine metabolism in wild type and TbMPC null mutant cell lines were investigated using  $^1\text{H}$ -NMR spectrometry, which facilitates a quantitative comparison, as previously described (Millerioux *et al.*, 2012; Bringaud *et al.*, 2015). PCF were incubated in PBS containing 4 mM [ $\text{U-}^{13}\text{C}$ ]glucose in the presence or absence of 4 mM threonine prior to  $^1\text{H}$ -NMR quantification of the end products excreted from these carbon sources. In this experiment, threonine-derived acetate production was used as a reference to estimate the impact of *tbmpc* gene deletion on pyruvate-dependent acetate production, as threonine in the incubation buffer served as a substrate for the pyruvate-independent acetate production by threonine degradation pathway (Millerioux *et al.*, 2013). The amount of glucose consumed during the incubation was determined under these conditions and was found to be similar in all three cell lines: 3.33  $\pm$  0.36, 3.44  $\pm$  0.63 and 3.89  $\pm$  0.11  $\mu\text{mol}$  in wild type, *Δtbmpc1*-B6 and *Δtbmpc2*-2C4, respectively [mean of 4 or 5 biological replicates  $\pm$  standard deviation (SD)].

Direct visual comparison of cells incubated with and without threonine, irrespective of the cell line, revealed slightly lower motility in samples without threonine, although the cells in all samples were viable at the end of the incubation. Production of  $^{13}\text{C}$ -enriched acetate, pyruvate and alanine from [ $\text{U-}^{13}\text{C}$ ]glucose and production of nonenriched acetate from threonine were quantified for the three cell lines studied (wild type, *Δtbmpc1*-B6 and *Δtbmpc2*-2C4; Table 2). No succinate was

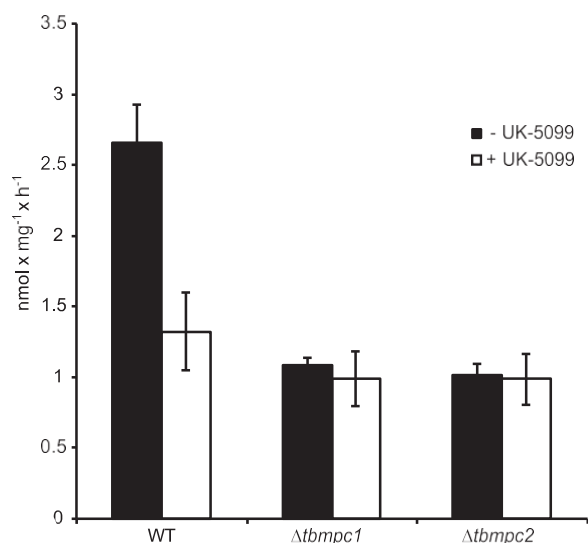


**Fig. 3.** Effect of the *tbmpc1* deletion and MPC inhibition by UK-5099 on pyruvate import into isolated PCF mitochondria. The import of radiolabeled pyruvate was decreased in *Δtbmpc1*-B6 and *Δtbmpc2*-2C4 compared with wild type samples. The import of pyruvate in the *Δtbmpc1*-B6 and *Δtbmpc2*-2C4 mutants was not affected using the MPC specific inhibitor UK5099, while import was reduced twofold in wild type cells. The error bars indicate standard deviations of three independent experiments.

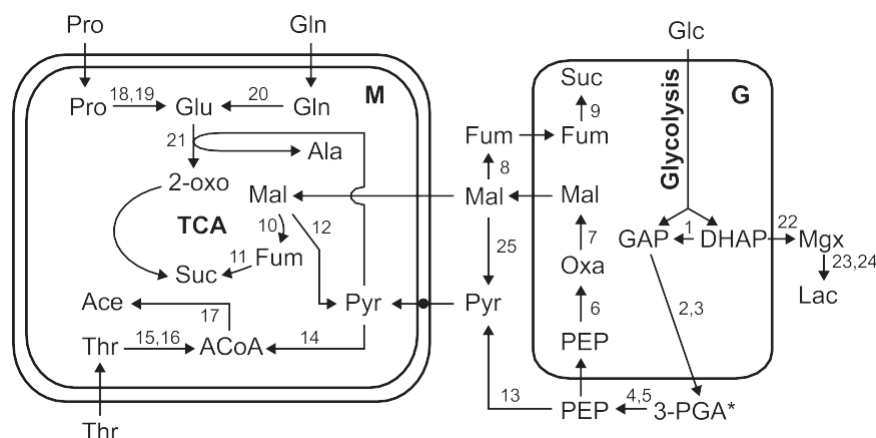


**Fig. 4.** Simplified metabolic scheme of *T. brucei*. A metabolic scheme depicting the fate of glucose (Glc) and the amino acids threonine (Thr), proline (Pro) and glutamine (Gln). Glucose is eventually converted to cytosolic 3-phosphoglycerate (3-PGA; \* - in case of procyclic cells, 1,3-bisphosphoglycerate is exported from glycosomes) through glycolysis within glycosomes (G) and further oxidized to phosphoenolpyruvate (PEP) in the cytosol. A part of PEP is transported back to G and metabolized to oxaloacetate (Oxa). Oxa is converted to malate (Mal), a branch-point intermediate that can be converted to pyruvate (Pyr) or to fumarate (Fum) in the cytosol, leading to the formation of succinate (Suc) in G, or transported to the mitochondrion (M), where this molecule enters the incomplete tricarboxylic acid cycle (TCA) or is converted to Pyr. The remaining PEP is converted to Pyr, which is either excreted or transported through MPC (full circle) into M. In the mitochondrial matrix, Pyr and Thr are metabolized to acetyl CoA (ACoA), which is subsequently catabolized to acetate (Ace). Both Pro and Gln are converted to glutamate (Glu), which enters the TCA cycle upon transamination with Pyr, yielding alanine (Ala) and 2-oxoglutarate (2-oxo). 2-Oxo is metabolized to mitochondrial succinate (Suc) through TCA enzymes in PCF. During the course of glycolysis, most of dihydroxyacetone phosphate (DHAP) is converted to glyceraldehyde phosphate (GAP), while a minor part of DHAP is spontaneously dephosphorylated to methylglyoxal (Mgx). This harmful compound is then detoxified to L-lactate (Lac). The following enzymes are shown: 1 - triose phosphate isomerase; 2 - glyceraldehyde phosphate dehydrogenase; 3 - phosphoglycerate kinase; 4 - phosphoglyceromutase; 5 - enolase; 6 - phosphoenolpyruvate carboxykinase; 7 - malate dehydrogenase; 8 - cytosolic fumarase; 9 - glycosomal fumarate reductase; 10 - mitochondrial fumarase; 11 - mitochondrial fumarate reductase; 12 - mitochondrial malic enzyme; 13 - pyruvate kinase; 14 - pyruvate dehydrogenase; 15 - threonine dehydrogenase; 16 - 2-amino-3-ketobutyrate coenzyme A ligase; 17 - acetate:succinate CoA-transferase; 18 - L-proline dehydrogenase; 19 - pyrroline-5-carboxylate dehydrogenase; 20 - glutaminase; 21 - L-alanine aminotransferase; 22 - nonenzymatic phosphate elimination; 23 - methylglyoxal reductase; 24 - lactaldehyde dehydrogenase; 25 - cytosolic malic enzyme.

detected, likely reflecting the absence of  $\text{NaHCO}_3$  in the incubation buffer, which was used to support the flux towards the mitochondrial oxidation of pyruvate at the expense of the downregulation or suppression of the succinate fermentation branch. Consistent with the results of the HPLC analysis, both mutant cell lines produced elevated levels of pyruvate and decreased levels

of glucose-derived acetate compared to wild type cells, regardless of the presence of threonine (Table 2). In the presence of threonine, alanine production from glucose was observed in wild type and mutant cell lines, whereas in the absence of threonine, relatively small amounts of alanine were only detected in TbMPC null mutants.

**Table 1.** Effect of *mpc1* and *mpc2* gene deletion, PEPCCK downregulation and presence of the pyruvate transporter inhibitor (UK-5099) on the production of metabolic end products in PCF cell lines.

		Metabolic end product Average6 SD [nmol 3 h <sup>-1</sup> 3 mg protein <sup>-1</sup> ] (fraction of total metabolites detected)					
Cell line	n	Pyruvate	Succinate	Lactate	Acetate	Fumarate	Total
Parental	6	32 6 5 (4%)	325 6 19 (45%)	42 6 2 (6%)	325 6 10 (45%)	1.25 6 0.24 (0.17%)	726 6 36
Parental 1 UK5099	3	74 6 1 (13%)	256 6 3 (44%)	21 6 2 (4%)	235 6 7 (40%)	1.10 6 0.03 (0.19%)	588 6 12
<sup>RNAi</sup> PEPCK	3	6 6 0 (2%)	56 6 5 (22%)	38 6 4 (15%)	155 6 23 (61%)	0.18 6 0.02 (0.07%)	255 6 32
<i>Dtbmpc1</i> -B6	6	122 6 13 (23%)	236 6 28 (45%)	14 6 3 (3%)	153 6 17 (29%)	1.06 6 0.10 (0.20%)	527 6 51
<i>Dtbmpc1</i> -B6 1 UK5099	3	95 6 3 (19%)	225 6 16 (44%)	17 6 1 (3%)	173 6 8 (34%)	0.86 6 0.09 (0.17%)	511 6 28
<i>Dtbmpc2</i> -2C4	6	135 6 16 (24%)	247 6 12 (44%)	14 6 2 (2%)	169 6 8 (30%)	1.50 6 0.27 (0.27%)	565 6 29
<i>Dtbmpc2</i> -2C4 1 UK5099	3	106 6 2 (20%)	240 6 2 (44%)	15 6 1 (3%)	178 6 1 (34%)	1.28 6 0.07 (0.24%)	541 6 2
<i>Dtbmpc1</i> -B6/ <sup>RNAi</sup> PEPCK	3	53 6 4 (28%)	57 6 8 (31%)	15 6 3 (8%)	62 6 6 (33%)	0.27 6 0.00 (0.15%)	187 6 21

Metabolic end products were determined by HPLC.  $n \geq 3$ ; The detected differences in metabolites are statistically significant as evaluated using the Kruskal-Wallis test with  $\alpha \leq 0.05$ .

**Table 2.** NMR determination of metabolic end products from glucose (Glc) and L-threonine (Thr) in PCF with deleted *mpc1* and *mpc2* genes.

Cell line	Metabolic end products from different substrates Average $\pm$ SD [nmol 3 h <sup>-1</sup> 3 mg protein <sup>-1</sup> ]									
	Glucose				Glucose 1 Threonine (Glc 1 Thr)					
	Pyruvate	Alanine	Acetate	Total	Pyruvate Glc	Alanine Glc	Acetate		Total	
							Glc	Thr	Glc	Thr
Parental	127 6 48	0	1152 6 146	1280 6 193	433 6 76	210 6 58	1101 6 97	2816 6 204	1744 6 178	2816 6 204
<i>Dtbmpc1</i> -B6	1064 6 62	67 6 48	252 6 50	1383 6 70	1738 6 200	270 6 47	407 6 46	3197 6 243	2415 6 219	3197 6 243
<i>Dtbmpc2</i> -2C4	1037 6 40	108 6 30	207 6 58	1352 6 83	1745 6 36	336 6 59	350 6 54	2443 6 87	2432 6 100	2443 6 87

*n* 5. The detected differences in metabolites are statistically significant as evaluated using the Kruskal-Wallis test with  $\alpha$  5 0.05.

The preference for threonine over glucose for the generation of acetate (approximately 2.6:1) was documented in wild type samples. This ratio was further increased in both null mutants [approximately 7.9:1 and 7.0:1 in *Dtbmpc1*-B6 and *Dtbmpc2*-2C4 cells, respectively (Table 2)], consistent with the expected decrease in pyruvate import into the mitochondrion. The NMR analysis showed that acetate production from glucose, through the pyruvate-dependent pathway, was reduced approximately threefold and fivefold in the TbMPC null mutants in the presence and absence of threonine, respectively. Clearly TbMPC is involved in acetate production from pyruvate; however, the significant residual acetate production from glucose implies that an alternative route is used in PCF trypanosomes.

#### Rearrangement of metabolism in *Dtbmpc1*-B6 PCF upon knockdown of PEPCK

Glucose-derived malate enters the mitochondrion and serves as a substrate for the mitochondrial malic enzyme (mitME) in a reaction yielding pyruvate (Allmann *et al.*, 2013). We suppressed this pathway in PCF wild type and *Dtbmpc1*-B6 cell lines by RNAi targeting phosphoenolpyruvate carboxykinase (PEPCK) to distinguish the contribution of TbMPC1-dependent pyruvate transport and malate-dependent pyruvate production to the formation of acetate. Downregulation of PEPCK expression in <sup>RNAi</sup>PEPCK and *Dtbmpc1*-B6/<sup>RNAi</sup>PEPCK samples was examined using Western blotting with an anti-PEPCK antibody (Supporting Information Fig. S3). Clones A11 (<sup>RNAi</sup>PEPCK) and C5 (*Dtbmpc1*-B6/<sup>RNAi</sup>PEPCK) were selected for further experiments. No PEPCK signal was detected in either clone, allowing us to assume that PEPCK downregulation was efficient. To avoid the appearance of revertants of constitutive RNAi, freshly selected cells were used in the assays. The growth of PCF 427, *Dtbmpc1*-B6, <sup>RNAi</sup>PEPCK and *Dtbmpc1*-B6/<sup>RNAi</sup>PEPCK cell lines in standard SDM79 was comparable (Supporting Information Fig. S3). The end products of glucose metabolism were analyzed using

HPLC in knockdown, parental and the *Dtbmpc2*-2C4 cell lines (Table 1). The production of succinate and fumarate was reduced in both RNAi cell lines, reflecting the partial inhibition of the succinate fermentation pathway. Acetate production was decreased in the <sup>RNAi</sup>PEPCK and *Dtbmpc1*-B6/<sup>RNAi</sup>PEPCK cell lines compared with the parental wild type and *Dtbmpc1*-B6 cell lines, respectively, as previously described for the *Dpepck* mutant (Ebikeme *et al.*, 2010). However, relative acetate production was similar in *Dtbmpc1*-B6, *Dtbmpc2*-2C4 and *Dtbmpc1*-B6/<sup>RNAi</sup>PEPCK cell lines (29-33% of the excreted end products from glucose metabolism; Table 1). The same relative production of acetate, regardless of PEPCK expression, strongly suggests that the contribution of malate to mitochondrial pyruvate metabolism is not significant. Alternatively, the activation of a third unknown adaptive route in the double mutant cannot be excluded.

#### Analysis of the *Dtbmpc1* BSF mutant cell line

The *tbmpc1* gene was deleted in the 427 BSF strain. The deletion of both alleles in several clones was confirmed by Southern blot analysis, and clone 2 (*Dtbmpc1*-2) was selected for further experiments (Fig. 2C). Knock-in BSF strains expressing epitope-tagged TbMPC1 in *Dtbmpc1*-2 as well as wild type background were generated and the expression of TbMPC1-HA was confirmed by Western blotting (Fig. 2D). Interestingly, the *Dtbmpc1*-2 BSF cell line did not exhibit any growth defect when cultured in complex HMI-9 medium (Fig. 2E), whereas the growth of this mutant was not supported in the recently developed Creek's minimal culture medium (CMM) (Creek *et al.*, 2013) (Fig. 2F). Growth rates were calculated from data within the linear sections of the curves (96-168 h post introduction to CMM), showing that the growth rate of the deletion mutant reached 36% (relative SD 5 1.6%, *n* 5 3) of the wild type cell line (100%, SD 5 6.2%, *n* 5 3). Partial complementation of the growth phenotype was observed in the knock-in cell line in *Dtbmpc1*-2 background (75%,



SD 5 2.2%,  $n$  5 3; Fig. 2F). Following the observation of *Dtbmpc1-2* growth defect in CMM, we checked whether *Dtbmpc1-2* showed altered mitochondrial membrane potential. Parental and *Dtbmpc1-2* cells were stained using tetramethylrhodamide ethyl ester and analyzed by flow cytometry using a published protocol (see Subrtova et al., 2015, and Supporting Information). No change in the potential was observed in cells cultured in either media (Mann-Whitney  $U$ -test 5 4;  $P$  5 1.0;  $n$  5 3 for both HMI-9 and CMM). Next, we attempted to supplement CMM with all individual components of HMI-9 which are missing in CMM (see Supporting Information Table S5 in Creek et al., 2015) at concentrations present in HMI-9. All individual supplements were tested in a pilot screen aimed at identifying a supplement which (i) would restore the growth of *Dtbmpc1-2* cell line in CMM and (ii) would not affect the growth of parental *T. brucei* Lister 427 BSF. The cells were diluted to  $2.3 \times 10^4$  cells per ml, aliquoted at 2 ml in culture plates and counted for 3 days after inoculation. HMI-9 and CMM were used as controls. No tested component of HMI-9 matched both requirements, leading us to the conclusion that the growth defect of *Dtbmpc1-2* in CMM is not caused by the lack of a single missing component present in HMI-9.

Because the *in vitro* growth of the *Dtbmpc1-2* BSF mutant in CMM was affected, we compared the development of infection in mice. All mice infected with wild type parasites died within 5 days of inoculation, whereas only two out of five *Dtbmpc1-2*-infected mice died within 10 days according to Kaplan-Meier survival curves (log F5 rank test 5 9.29;  $P < 0.01$ ; Fig. 5). Mice infected with the

that in BSF *T. brucei* TbMPC1 plays an important role *in vivo* and under specific conditions *in vitro*.

To study acetate production from glucose, the *Dtbmpc1-2*, *tbmpc1*<sup>-1</sup> (single allele mutant) and wild type BSF trypanosomes were incubated in PBS containing [ $^{13}\text{C}$ ]glucose and threonine for the  $^1\text{H}$ -NMR quantification of excreted end products, as previously described (Mazet et al., 2013; Creek et al., 2015). Apart from pyruvate, which represents ~85% of the end products excreted from glucose, alanine, acetate and lactate were detected using  $^1\text{H}$ -NMR. Differences in the levels of acetate produced from glucose and the ratio of threonine/glucose utilization for acetate production were observed. Similar to observations in PCF, the rate of glucose-derived acetate production was significantly decreased in the *Dtbmpc1-2* cell line (4.6-fold) compared to wild type cells. In addition, an intermediate situation was observed for the *tbmpc1*<sup>-1</sup> cell line with a 1.5-fold reduction of glucose-derived acetate production compared to wild type (Table 3). This effect shifted the ratio of threonine to glucose utilization for acetate production from approximately 0.8 in wild type cells to 1.3 and 3.7 in the *tbmpc1*<sup>-1</sup> and *Dtbmpc1-2* cell lines, respectively. As observed for the PCF mutants, the results of the NMR analyses are consistent with a role for TbMPC in pyruvate transport to the mitochondria in BSF trypanosomes.

## Discussion

In this study, we assign a pyruvate transport function to two MPC proteins (TbMPC1 and TbMPC2) in the parasitic protist *T. brucei*. We demonstrated that both MPC subunits localized in the mitochondrial membrane of PCF *T. brucei*, and we showed the importance of both subunits for pyruvate uptake using null mutant cell lines. We also addressed the adaptations of metabolic fluxes in MPC deletion mutants in both PCF and BSF trypanosomes and investigated the phenotype of BSF *tbmpc1* null mutants *in vivo* in mouse infections.

In the genome of *T. brucei*, we identified two MPC paralogs. MPC proteins are members of the Mtn3-like clan, bearing structural similarity to bacterial SemiSWEET proteins that mediate sugar transport (Vanderperre et al., 2014). Whereas the SemiSWEET transporter functions as a symmetrical dimer of triple-helix units, the pyruvate carrier is asymmetrical, comprising two TM helices of MPC1 and three TM helices of MPC2 (Bender et al., 2015). We analyzed the primary sequences of MPCs described thus far and TbMPCs, focusing on conserved amino acids implicated in SemiSWEET transport function. In all analyzed MPC proteins, a conserved tryptophan typical of the SemiSWEET binding pocket is present in MPC2 and substituted for phenylalanine in MPC1 proteins. However, it is unlikely

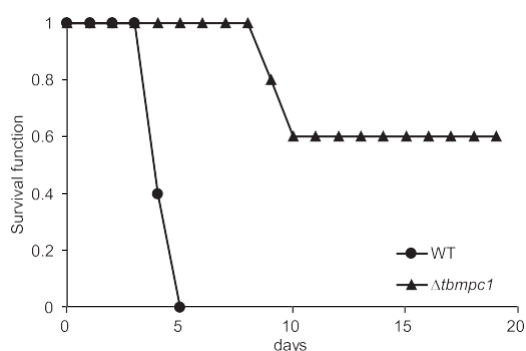


**Fig. 5.** Effect of the *tbmpc1* deletion in BSF on the viability of infected mice ( $n$  5 5). Survival analysis of wild type- (circles) and *Dtbmpc1-2*-infected mice (triangles).

**Table 3.** Effect of *mpc1* gene deletion (-/-) and single allele *mpc1* deletion (-/1) in BSF on the production of glucose-derived metabolic end products using NMR.

Cell line	Metabolic end products Average $\pm$ SD [nmol/3 h <sup>2</sup> $\times$ 3 mg protein <sup>2</sup> <sup>-1</sup> ]					
	Pyruvate Glc	Alanine Glc	Acetate		Total	
			Glc	Thr	Glc	Thr
Parental	13,277 $\pm$ 62076	1648 $\pm$ 6252	532 $\pm$ 6116	410 $\pm$ 689	15,686 $\pm$ 2384	410 $\pm$ 689
<i>Dtbmpc1</i> <sup>-/1</sup>	11,307 $\pm$ 62351	1381 $\pm$ 6292	354 $\pm$ 693	435 $\pm$ 6134	13,117 $\pm$ 62591	435 $\pm$ 6134
<i>Dtbmpc1-2</i> <sup>-/-</sup>	11,280 $\pm$ 61358	1240 $\pm$ 6256	116 $\pm$ 670	426 $\pm$ 6108	12,825 $\pm$ 61597	426 $\pm$ 6108

*n* 5-10. The values indicated in bold represent statistically significant differences in the production of a given metabolite as evaluated using the Kruskal-Wallis test, with  $\alpha$  5 0.05.

that this substitution affects the transport function of MPCs, as a corresponding tryptophan to phenylalanine mutation in the SemiSWEET transporter did not affect sucrose uptake through SemiSWEET proteins in a liposome assay (Lee *et al.*, 2015). The different number of transmembrane helices in SemiSWEET and MPC transporters results in differences in the binding pocket, which can explain the specificity of the transported substrates (sucrose uniport vs. pyruvate-proton symport). A rather surprising finding concerns the expected hinge region of TbMPC1. All other analyzed MPC1 subunits presented a conserved proline in the second TM helix, consistent with Lee *et al.* (2015), which serves as an important molecular hinge for the binder clip-like transition between inward-open and outward-open states of the transporter in SemiSWEET proteins and proteins from the PQ-loop family. A proline-to-alanine substitution in SemiSWEET at this site strongly diminishes sucrose transport (Lee *et al.*, 2015). The same substitution is present in TbMPC1. We propose that for the opening of TbMPC pore, it is sufficient for proline-induced intramolecular conformational changes to occur in only one protomer.

Both TbMPC1 and TbMPC2 proteins were localized to the mitochondria of PCF trypanosomes by indirect immunofluorescence, and the expression of both proteins was detected in mitochondrial membrane fractions. This result is consistent with previous finding of these proteins in the PCF mitochondrial proteome (Panigrahi *et al.*, 2009). The mitochondrial localization of TbMPC1 was also determined in BSF. No staining for TbMPC1 was detected at the BSF plasma membrane, precluding the involvement of MPC in the export of pyruvate as a metabolic end product. It has recently been reported that pyruvate export is mediated through distinct TbPT transporters (Sanchez, 2013). Although we were unable to express TbMPC2 in BSF, the localization of TbMPC2 in the BSF mitochondrion is conceivable based on the localization in PCF and the reported association of MPC1 with MPC2 in other species (Bricker *et al.*, 2012; Herzig *et al.*, 2012).

The essential function of both TbMPC1 and TbMPC2 for mitochondrial pyruvate transport was directly demonstrated by monitoring <sup>14</sup>C-pyruvate uptake in mitochondria isolated from PCF wild type and TbMPC null mutants. TbMPC-dependent pyruvate import accounted for the total inhibitor-sensitive import, consistent with observations in *S. cerevisiae* (Herzig *et al.*, 2012). Functional transport complexes were not detected in either *Dtbmpc1*-B6 or *Dtbmpc2*-2C4 cell lines, consistent with available data from yeast (Herzig *et al.*, 2012; Bender *et al.*, 2015).

The analysis of the metabolic end products in cell lines lacking either TbMPC subunit strengthened the notion that TbMPCs represent pyruvate transporters in PCF and BSF trypanosomes. Specifically, the decreased production of glucose-derived acetate in both BSF and PCF lacking one *tbmpc* gene most likely reflects a decreased intramitochondrial pyruvate concentration. However, some glucose-derived acetate is still produced in both PCF and BSF mutant cell lines, while acetate production from glucose is abolished in both BSF and PCF cell lines upon knock down of the subunit E2 of pyruvate dehydrogenase (<sup>RNAi</sup>PDH-E2) (Mazet *et al.*, 2013; Millerioux *et al.*, 2013). This finding supports the view that an alternative route is used in both trypanosome stages to produce/import glucose-derived pyruvate in the mitochondrion. According to the current model of PCF central metabolism, a significant part of the flux from glucose diverted to the glycosome for malate production is exchanged with the mitochondrion to produce pyruvate through mitME inside the mitochondrion (Allmann *et al.*, 2013). This hypothesis is consistent with the observed decrease in succinate production based on HPLC analysis in both PCF null mutants, as a higher proportion of malate would be used as a substrate for mitME to compensate for the lack of pyruvate transport through MPC, eventually leading to a decrease in succinate levels. To further address this hypothesis, we analyzed metabolic perturbations or adaptations in *Dtbmpc1*-B6/<sup>RNAi</sup>PEPCK and <sup>RNAi</sup>PEPCK

PCF cell lines in which the first step of the glycosomal succinate branch is downregulated. The control <sup>RNAi</sup>-PEPCK cell line showed a 2-fold reduction of acetate production compared to the wild type parasite, consistent with previous analyses of the *Dpepck* mutant (Ebikeme *et al.*, 2010). A similar reduction of the rate of acetate production was also observed in *Dtbmpc1-B6*/<sup>RNAi</sup>PEPCK compared to *Dtbmpc1* (2.5-fold). These data suggest that either the pathway comprising PEPCK, malate dehydrogenase and mitME contributes poorly to pyruvate/acetate production from glucose in the mitochondrion, or a third route is used in the *Dtbmpc1-B6*/<sup>RNAi</sup>PEPCK cell line, that is, MPC-independent mitochondrial pyruvate transport. Indeed, approximately 40% of the total pyruvate uptake was observed in mitochondria treated with UK-5099 and MPC knock-out cell lines, which is in favour of an alternative pyruvate transporter, such as a member of the monocarboxylate transporter family with broader specificity. Monocarboxylate transporters are typically present at the cell surface, but the mitochondrial localization of these proteins has been reported in rats and baker's yeast (Nalecz *et al.*, 1991; Butz *et al.*, 2004). However, it cannot be excluded that the mitochondrial membrane integrity of digitonin-permeabilized cells was partially affected in our experiments, facilitating the passive diffusion of <sup>14</sup>C-pyruvate into the mitochondrion. Clearly, additional experiments are required to understand how glucose-derived acetate is produced in *Dtbmpc* mutant cell lines.

The upregulation of TbMPC proteins in PCF was observed in two proteomic studies, with a fivefold upregulation for TbMPC1 and a fourfold upregulation for TbMPC2 according to Butter *et al.* (2013) and twofold upregulation for TbMPC1 according to Urbaniak *et al.* (2012). This finding is consistent with a higher proportion of glucose-derived pyruvate converted into acetate in PCF compared to BSF, representing up to 70% and 5% of the end products excreted from glucose metabolism, respectively (Mazet *et al.*, 2013; Bringaud *et al.*, 2015). As expected, no growth defect was apparent in either PCF *Dtbmpc1-B6* or *Dtbmpc2-2C4* cells *in vitro*, as the acetate production capacity was not impaired, that is, both mutant cell lines still produced acetate from glucose and threonine, the other source of acetate present in the growth medium.

In contrast to PCF trypanosomes, the MPC gene deletion seems to affect BSF metabolism because (i) the growth of the *Dtbmpc1-2* BSF cells was not supported in CMM minimal medium compared with the wild type cells, (ii) we were unable to either express or knock out TbMPC2 in BSF and (iii) the *Dtbmpc1-2* BSF mutant showed reduced lethality of infection in mice. Although pyruvate is the principal metabolic end product excreted

from glucose metabolism in BSF trypanosomes, the diminished pyruvate transport into the mitochondrion strongly affected this parasite, as an 80% reduction in acetate production was observed in the *Dtbmpc1-2* mutant (Table 3). In the mitochondrion, pyruvate is further oxidized by PDH, generating acetyl-CoA and eventually acetate. It was recently shown that PDH and threonine dehydrogenase (TDH) are synergistically essential for the growth of BSF in rich medium because of acetate production; both <sup>RNAi</sup>PDH-E2 and *Dtdh* single mutants remain viable under these conditions. Accordingly, the <sup>RNAi</sup>PDH-E2 cell line is lethal in the absence of threonine (Mazet *et al.*, 2013). Interestingly, the growth of the *Dtbmpc1* BSF mutant in CMM could not be rescued by threonine, suggesting that the observed reduction in acetyl-CoA or acetate production is not responsible for *Dtbmpc1-2* death. Alternatively, we hypothesize that MPC is necessary in BSF for supplying the substrate for mitochondrial alanine aminotransferase (AAT). It has been suggested that AAT catalyzing the transamination of pyruvate and glutamate into alanine and  $\alpha$ -ketoglutarate is essential in both PCF and BSF (Spitznagel *et al.*, 2009). No activity of the downstream enzyme,  $\alpha$ -ketoglutarate dehydrogenase, could be detected in bloodstream *T. brucei* (Sykes and Hajduk, 2013), suggesting that the essential function of AAT might not be directly connected to cellular metabolism. In this context, the question of availability of alanine for mitochondrial translation should be addressed: while it is well documented that mitochondrial translation is essential in both procyclic and bloodstream *T. brucei* (Cristodero *et al.*, 2010), information on amino acid import into the mitochondrion is very limited in *T. brucei* (de Macedo *et al.*, 2015) and surprisingly scarce in general (King, 2007).

In summary, we identified a mitochondrial pyruvate transporter comprising two subunits and described the properties and function of this protein in the metabolism of a human parasite and an important model organism, *T. brucei*. Furthermore, these data support the recently emerging picture of BSF functioning well beyond glycolysis, with unexpectedly active mitochondrial metabolic pathways (Roldan *et al.*, 2011; Mazet *et al.*, 2013; Creek *et al.*, 2015).

## Materials and methods

### *In silico* analyses

Putative *mpc1* and *mpc2* genes were identified using BLAST in the *T. brucei* genome database ([www.tri-trypdb.org](http://www.tri-trypdb.org)) (Aslett *et al.*, 2010). Both genes were aligned to 29 selected MPC homologs obtained by a

BLAST search using *S. cerevisiae* MPCs as queries using Muscle 3.8.425 software (default parameters) (Edgar, 2004) and trimmed with BMGE 1.12 (-b 1 -m BLOSUM30) (Criscuolo and Gribaldo, 2010). The protein evolution model was selected using ProtTest 3.2 (Darriba *et al.*, 2011). PhyML 2.2.0 (topology search: best of NNIs and SPRs, initial tree: BioNJ, Substitution model: LG, proportion of invariable sites: fixed (0), gamma distribution parameter: estimated; number of categories: 4; bootstrap replicates: 500) (Guindon and Gascuel, 2003) and MrBayes 3.2.2 (rate matrix: LG; rate variation: gamma; gamma categories: 4; chain length: 2,000,000; heated chains: 4; heated chain temp: 0.2; burn-in length: 500,000) (Huelsenbeck and Ronquist, 2001) were used to reconstruct the phylogenetic tree. Transmembrane domains were predicted using the TMHMM Server 2.0 (Krogh *et al.*, 2001) and TMPred (Hofmann and Stoffel, 1993). MitoProt (Claros and Vincens, 1996) and PSORTII (Nakai and Horton, 1999) were used to predict subcellular localization.

#### Cell cultivation

*T. brucei* PCF strains 427 and 29-13 (expressing TetR and T7RNAP) (Wirtz *et al.*, 1999) were grown at 27°C in SDM-79 medium (Brun and Schonenberger, 1979) supplemented with 10% (v/v) fetal calf serum. *T. brucei* BSF 427 and New York Single Marker (SM, expressing TetR and T7RNAP) (Wirtz *et al.*, 1999) strains of the same species were grown in HMI-9 medium supplemented with 10% (v/v) fetal calf serum (Hirumi and Hirumi, 1989) or CMM supplemented with 10% (v/v) fetal calf serum (Creek *et al.*, 2013) at 37°C in 5% CO<sub>2</sub>. PCF 29-13 *T. brucei* were grown in the presence of hygromycin (25 lg/ml) and G418 (15 lg/ml), BSF SM cells were grown in the presence of G418 (1.5 lg/ml). The following concentrations were used for additional antibiotics in cultures of PCF cell lines after transformation: 1 lg/ml of puromycin, 2.5 lg/ml of phleomycin and 10 lg/ml of blasticidin. For BSF mutant cell lines, puromycin at 0.1 lg/ml, blasticidin at 5 lg/ml and phleomycin at 2.5 lg/ml were used. A Z2 cell counter (Beckman Coulter, USA) was used to count the growing trypanosome cultures. The cells were maintained at the exponential growth phase (PCF and BSF were diluted daily to  $2.3 \times 10^6$  and  $1.3 \times 10^4$ , respectively), and cumulative cell numbers were calculated.

#### Generation of mutant cell lines

Tagged TbMPC1 and TbMPC2 were expressed in PCF 29-13 and BSF SM trypanosomes. The entire *tbmpc1* ORF was PCR-amplified from PCF Tb427 gDNA using

the appropriate primers (see Supporting Information Table S1) and subcloned into plasmid pT7-3V5-PAC (Flaspohler *et al.*, 2010) with a C-terminal V5 tag and a puromycin resistance marker. Plasmid pJH54, with a triple HA tag bearing the phleomycin resistance marker (derived from pLEW100; a kind gift from C. Clayton, University of Heidelberg, Germany), was used for

expression of whole *tbmpc2* ORF.

To generate *tbmpc1* and *tbmpc2* null mutants, the 5'- and 3'-flanking regions of *tbmpc1* and *tbmpc2* ORFs were PCR amplified (see Supporting Information Table S1 for primers) and sequentially inserted into the plasmids pBS-blast and pBS-phleo (Ruepp *et al.*, 1997), resulting in four plasmids in which the genes encoding blasticidin deaminase or bleomycin binding protein were flanked by 5' and 3'UTRs of TbMPC1 or TbMPC2. Two rounds of transformation and selection were required to obtain *Dtbmpc1* and *Dtbmpc2* clonal cell lines.

Knock-in BSF strains expressing TbMPC1-HA in *Dtbmpc1-2* as well as wild type background were generated using the plasmid pHD1034 (Quijada *et al.*, 2002). Puromycin was used to select stable transformants and the ectopic expression of tagged TbMPC1 driven by an rRNA promoter was checked by Western blotting with a mouse monoclonal anti-HA-tag antibody (Sigma-Aldrich, USA).

To generate cell lines showing the constitutively downregulated expression of PEPCK, a sense-antisense fragment, comprising the 3' portion of PEPCK (Tb927.2.4210) coding sequence and the beginning of the 3'UTR of PEPCK, was excised from an existing vector (Coustou *et al.*, 2008) and inserted in pHD1034 to generate the PEPCK RNAi vector. Wild type and *Dtbmpc1-B6* PCF cell lines were used as parental cell lines for the transformations. The downregulation of PEPCK expression in both resulting cell lines was evaluated through Western blotting with an anti-PEPCK antibody (a kind gift from Thomas Sebeck, University of Bern, Switzerland).

Linearized plasmids were electroporated into parental PCF *T. brucei* using two subsequent pulses (1500 V and 1700 V) with a Gene Pulser Xcell (Bio-Rad, USA) (Vondruskova *et al.*, 2005), or parental BSF was transfected using an Amaxa Nucleofector (Lonza, Switzerland) (Burkard *et al.*, 2011), respectively. The transformed cells were subjected to limiting dilution. The growth of PCF clones was facilitated using parental feeder cells in conditioned medium and a 5% CO<sub>2</sub> atmosphere (pouches with CO<sub>2</sub> gen compact, Oxoid).

#### Southern blotting

Genomic DNA was isolated from cultures of BSF *T. brucei* 427 and *Dtbmpc1-2* strains using the TELT method (Medina-Acosta and Cross, 1993) and digested with



BamHI or EcoRV enzymes. Approximately 10 lg of digested gDNA was loaded per well. Gel electrophoresis and Southern blotting was performed using standard procedures (Southern, 2006). Digoxigenin-labeled probes for the complete coding sequences of TbMPC1 and blasticidine deaminase were prepared using the PCR DIG Probe Synthesis Kit (Roche) with the primers listed in Supporting Information Table S1. Hybridization was conducted using DIG Easy Hyb buffer at 42°C. Washing and blocking buffers and anti-digoxigenin-alkaline phosphatase with CSPD as substrate were purchased from Roche. Chemiluminiscent signal was detected on ImageQuant LAS4000 (GE Healthcare).

### Fluorescence microscopy

Approximately 2–3 × 10<sup>6</sup> PCF and BSF trypanosomes were used per slide. The PCF cells were incubated with 0.5 lM Mitotracker Red CMXRos (Life Technologies, USA) for 10 min in SDM-79 at 27°C, washed with phosphate-buffered saline (PBS), incubated in SDM-79 media for another 20 min and subsequently washed with PBS. The cells were fixed and permeabilized on the slides using -20°C cold methanol for 5 min, followed by 5 min incubation in -20°C cold acetone.

BSF trypanosomes were incubated with 25 nM Mitotracker Red CMXRos for 30 min in HMI-9 in 37°C, collected by centrifugation and incubated again for 10 min in HMI-9, followed by washing with PBS. The cells were fixed on slides using 3.6% formaldehyde for 15 min at room temperature, washed with PBS and permeabilized using 0.1% Triton X-100 for 10 min.

The slides were incubated in blocking solution (0.25% bovine serum albumin, 0.25% gelatin and 0.05% Tween 20 in PBS) for 1 h at room temperature. Expressed TbMPC1-V5 and TbMPC2-HA were visualized using mouse monoclonal anti-V5-tag and anti-HA-tag antibodies, respectively (both from Sigma-Aldrich, USA), and a secondary donkey anti-mouse Alexa Fluor 488 antibody (Life Technologies, USA). The cells were mounted in Vectashield with DAPI (Vector Laboratories, USA) and observed using an Olympus IX81 microscope. The images were captured using a Hamamatsu Orca-AG digital camera and processed using cell<sup>^</sup>R imaging software (Olympus, Japan).

### Infection of mice

Female 8-week-old Balb/c mice (*n* = 5) were intraperitoneally infected with 5–3 × 10<sup>4</sup> BSF trypanosomes. Prior to inoculation, the cells were harvested in mid-log phase from HMI-9 medium and washed once in PBS. Parasitemia was counted in Diff-Quik-stained (Medion Diagnos-

tics, USA) smears prepared from the tail blood of infected mice. Animal handling was approved by the Czech Ministry of Agriculture (53407/ENV/13-2300/630/13). The acquired data were analyzed by Kaplan-Meier survival analysis in MedCalc (MedCalc Software).

### Cell fractionation

Crude mitochondrial fractions were obtained through digitonin solubilization according to Smid *et al.* (2006). The integrity of the mitochondria and purity of the fractions were assessed after measuring activities of the cytosolic enzyme pyruvate kinase and the mitochondrial enzyme threonine dehydrogenase as markers for cytosolic and mitochondrial fractions, respectively. The extent of cross-contamination of the fractions was consistently below 2%. The mitochondrial membrane and matrix fractions were isolated using digitonin according to Mach *et al.* (2013).

To localize expressed recombinant TbMPC1 and TbMPC2 proteins, individual cell fractions were separated using SDS-PAGE, followed by Western blotting and visualization using mouse monoclonal anti-V5-tag and anti-HA-tag antibodies, respectively, and peroxidase-conjugated goat anti-mouse IgG (Sigma-Aldrich, USA). The purity of fractions was evaluated using antibodies against mitochondrial matrix (HSP60), mitochondrial membrane (porin) and cytosolic (enolase) marker proteins, kind gifts of S.L. Hajduk (University of Georgia, USA), M. Chaudhuri (Meharry Medical College, USA) and P. Michels (Catholic University of Louvain, Belgium), respectively.

### Pyruvate uptake

Uptake of radioactively labeled pyruvate was performed with digitonin-solubilized cells. Pyruvate stock solution was prepared after mixing nine volumes of 2 mM cold pyruvate with one volume of 2 mM [2-<sup>14</sup>C]-labeled pyruvate (ARC, USA). Following solubilization, the cell pellets (3.5 mg; equivalent of 5–6 × 10<sup>8</sup> cells) were stored on ice. For pyruvate import, the pellet was resuspended in 200 l of mannitol buffer, pH 7.4 (650 mM mannitol, 50 mM potassium phosphate, 1 mM EGTA, 0.1% BSA, 10 mM MgSO<sub>4</sub> and 1 mM ATP), and incubated on ice for 5 min. Next, the samples were pelleted and resuspended in 200 l of mannitol buffer, pH 6.3, containing 200 lM UK-5099 [alpha-cyano-beta-(2-phenylindol-3-yl)acrylate] or the same volume of DMSO (2 l) for 2 min at 27°C. Subsequently, 100 lM pyruvate diluted from the stock solution was added, and the samples were incubated at 27°C for 15 min. The reaction was quenched after the addition of 1 ml ice-cold mannitol



844 buffer, pH 7.4, containing 10 mM pyruvate. The perme-  
 845 abilized cells were washed four times in quenching  
 846 buffer and resuspended in 1 ml AquaLuma (Lumac Sys-  
 847 tems, USA) for scintillation counting.

#### 848 *Analysis of excreted end products from metabolism of* 849 *carbon sources*

850 High-performance liquid chromatography (HPLC) and  
 851 nuclear magnetic resonance (NMR) were used to iden-  
 852 tify and quantify the end products of glucose or L-threo-  
 853 nine metabolism.

854 HPLC analysis was performed using on a Hi-Plex H  
 855 column (300 3 7.7 mm, 8 l m) (Polymer laboratories,  
 856 USA) at 65°C and a flow rate of 0.4 ml/min, using 5 mM  
 857 H<sub>2</sub>SO<sub>4</sub> as eluent. The amount of the metabolite was  
 858 quantified as absorbance at 205 nm. The system was  
 859 calibrated by 5-point external calibration curves of differ-  
 860 ent concentrations of metabolites expected to be pres-  
 861 ent in the samples. The samples were prepared using  
 862 the following method: 10<sup>8</sup> trypanosomes per sample  
 863 were collected through centrifugation, washed and  
 864 resuspended in glucose incubation buffer (PBS with  
 865 24 mM NaHCO<sub>3</sub> and 10 mM glucose, pH 7.3) with 10  
 866 l M UK-5099 or the same volume of DMSO (2 l l) to final  
 867 volume of 200 l l and incubated for 2 h at 27°C. Subse-  
 868 quently, the cells were centrifuged, and the supernatant  
 869 was filtered through a 0.22-mm filter and 30 l l was  
 870 loaded onto the HPLC column. The output was visual-  
 871 ized and analyzed using Clarity 5 software (DataApex).

872 NMR analyses of end products excreted from glucose  
 873 and/or threonine metabolism were performed according  
 874 to Millerioux *et al.* (2013) for PCF and Mazet *et al.*  
 875 (2013) for BSF. *T. brucei* PCF (5.3 10<sup>7</sup>) or BSF  
 876 (2.53 10<sup>7</sup>) cells were collected after centrifugation at  
 877 1400 g for 10 min, washed once with phosphate-  
 878 buffered saline (PBS) containing 4 mM glucose (BSF) or  
 879 no glucose (PCF) and incubated for 6 h at 27°C (PCF)  
 880 or 5 h at 37°C (BSF) in 2.5 ml of PBS buffer (pH 7.4)  
 881 containing 4 mM [U-<sup>13</sup>C]glucose in the presence or  
 882 absence of 4 mM threonine. The integrity of the cells  
 883 during the incubation was assessed through microscopic  
 884 observation. The supernatant was collected, and 50 ml  
 885 of maleate solution in D<sub>2</sub>O (20 mM) was added as an  
 886 internal reference. <sup>1</sup>H-NMR spectra were performed at  
 887 125.77 MHz using a Bruker DPX500 spectrometer  
 888 equipped with a 5 mm broadband probe head. Measure-  
 889 ments were recorded at 25°C using the ERETIC  
 890 method. This method provides an electronically synthe-  
 891 sized reference signal. The following acquisition condi-  
 892 tions were used: 90° flip angle, 5000 Hz spectral width,  
 893 32 K memory size and 9.3 sec total recycle time. Meas-  
 894 urements were performed with 256 scans for a total

time close to 40 min. Prior to each experiment, the  
 phase of the ERETIC peak was precisely adjusted.  
 Resonances of the obtained spectra were integrated,  
 and the results were expressed relative to ERETIC peak  
 integration. The linear production of end products of  
 metabolism of [U-<sup>13</sup>C]-glucose (<sup>13</sup>C-enriched pyruvate  
 and acetate) throughout the experiment was confirmed  
 by H-NMR quantification of the end products excreted  
 by the wild type trypanosomes incubated for 6 h in PBS  
 containing 4 mM [U-<sup>13</sup>C]-glucose.

#### Acknowledgements

The authors would like to thank C. Clayton, University of Hei-  
 delberg, Germany, and I. Roditi, University of Bern, Switzer-  
 land, for plasmids, and T. Seebeck, University of Bern,  
 Switzerland, S.L. Hajduk, University of Georgia, USA, M.  
 Chaudhuri, Meharry Medical College, USA, and P. Michels,  
 Catholic University of Louvain, Belgium, for antibodies. The  
 authors would also like to thank Ivan Hrdý for consulting  
 throughout the study and Michaela Marcinková for excellent  
 technical assistance. This work was financially supported  
 through grants from the Biomedicine Centre of the Academy  
 of Sciences and Charles University (CZ.1.05/1.1.00/02.0109)  
 from the European Regional Development Fund, project  
 CZ.1.07/2.3.00/30.0061 from the European Social Fund, the  
 Centre National de la Recherche Scientifique (CNRS), the  
 Université de Bordeaux, the Agence Nationale de la Recher-  
 che (ANR) through grant ACETOTRYP of the ANR-BLANC-  
 2010 and the Laboratoire d'Excellence (LabEx) ParaFrap  
 ANR-11-LABX-0024.

#### References

- Allmann, S., Morand, P., Ebikeme, C., Gales, L., Biran, M.,  
 Hubert, J., *et al.* (2013) Cytosolic NADPH homeostasis in  
 glucose-starved procyclic *Trypanosoma brucei* relies on  
 malic enzyme and the pentose phosphate pathway fed  
 by gluconeogenic flux. *J Biol Chem* 288: 18494-18505.  
 Aslett, M., Aurrecoechea, C., Berriman, M., Brestelli, J.,  
 Brunk, B.P., Carrington, M., *et al.* (2010) TriTrypDB: a  
 functional genomic resource for the Trypanosomatidae.  
*Nucleic Acids Res* 38: D457-D462.  
 Bender, T., Pena, G., and Martinou, J.C. (2015) Regulation  
 of mitochondrial pyruvate uptake by alternative pyruvate  
 carrier complexes. *EMBO J* 34: 911-924.  
 Bricker, D.K., Taylor, E.B., Schell, J.C., Orsak, T., Boutron,  
 A., Chen, Y.C., *et al.* (2012) A mitochondrial pyruvate car-  
 rier required for pyruvate uptake in yeast, *Drosophila*,  
 and humans. *Science* 337: 96-100.  
 Bringaud, F., Biran, M., Millerioux, Y., Wargnies, M.,  
 Allmann, S., and Mazet, M. (2015) Combining reverse  
 genetics and NMR-based metabolomics unravels  
 trypanosome-specific metabolic pathways. *Mol Microbiol*  
 96: 917-926.  
 Brun, R., and Schonenberger (1979) Cultivation and in vitro  
 cloning or procyclic culture forms of *Trypanosoma brucei*

- in a semi-defined medium. Short communication. *Acta Trop* 36: 289-292.
- Burkard, G.S., Jutzi, P., and Roditi, I. (2011) Genome-wide RNAi screens in bloodstream form trypanosomes identify drug transporters. *Mol Biochem Parasitol* 175: 91-94.
- Butter, F., Bucerius, F., Michel, M., Cicova, Z., Mann, M., and Janzen, C.J. (2013) Comparative proteomics of two life cycle stages of stable isotope-labeled *Trypanosoma brucei* reveals novel components of the parasite's host adaptation machinery. *Mol Cell Proteomics* 12: 172-179.
- Butz, C.E., McClelland, G.B., and Brooks, G.A. (2004) MCT1 confirmed in rat striated muscle mitochondria. *J Appl Physiol* (1985) 97: 1059-1066.
- Claros, M.G., and Vincens, P. (1996) Computational method to predict mitochondrially imported proteins and their targeting sequences. *Eur J Biochem* 241: 779-786.
- Coustou, V., Biran, M., Breton, M., Guegan, F., Riviere, L., Plazolles, N., et al. (2008) Glucose-induced remodeling of intermediary and energy metabolism in procyclic *Trypanosoma brucei*. *J Biol Chem* 283: 16342-16354.
- Creek, D.J., Nijagal, B., Kim, D.H., Rojas, F., Matthews, K.R., and Barrett, M.P. (2013) Metabolomics guides rational development of a simplified cell culture medium for drug screening against *Trypanosoma brucei*. *Antimicrob Agents Chemother* 57: 2768-2779.
- Creek, D.J., Mazet, M., Achcar, F., Anderson, J., Kim, D.H., Kamour, R., et al. (2015) Probing the metabolic network in bloodstream-form *Trypanosoma brucei* using untar-getted metabolomics with stable isotope labelled glucose. *PLoS Pathog* 11: e1004689.
- Criscuolo, A., and Gribaldo, S. (2010) BMGE (Block Mapping and Gathering with Entropy): a new software for selection of phylogenetic informative regions from multiple sequence alignments. *BMC Evol Biol* 10: 210.
- Cristodero, M., Seebeck, T., and Schneider, A. (2010) Mitochondrial translation is essential in bloodstream forms of *Trypanosoma brucei*. *Mol Microbiol* 78: 757-769.
- Darriba, D., Taboada, G.L., Doallo, R., and Posada, D. (2011) ProtTest 3: fast selection of best-fit models of protein evolution. *Bioinformatics* 27: 1164-1165.
- Ebikeme, C., Hubert, J., Biran, M., Gouspillou, G., Morand, P., Plazolles, N., et al. (2010) Ablation of succinate production from glucose metabolism in the procyclic trypanosomes induces metabolic switches to the glycerol 3-phosphate/dihydroxyacetone phosphate shuttle and to proline metabolism. *J Biol Chem* 285: 32312-32324.
- Edgar, R.C. (2004) MUSCLE: multiple sequence alignment with high accuracy and high throughput. *Nucleic Acids Res* 32: 1792-1797.
- Finn, R.D., Bateman, A., Clements, J., Coghill, P., Eberhardt, R.Y., Eddy, S.R., et al. (2014) Pfam: the protein families database. *Nucleic Acids Res* 42: D222-D230.
- Flaspohler, J.A., Jensen, B.C., Saveria, T., Kifer, C.T., and Parsons, M. (2010) A novel protein kinase localized to lipid droplets is required for droplet biogenesis in trypanosomes. *Eukaryot Cell* 9: 1702-1710.
- Greig, N., Wyllie, S., Patterson, S., and Fairlamb, A.H. (2009) A comparative study of methylglyoxal metabolism in trypanosomatids. *FEBS J* 276: 376-386.
- Guindon, S., and Gascuel, O. (2003) A simple, fast, and accurate algorithm to estimate large phylogenies by maximum likelihood. *Syst Biol* 52: 696-704.
- Halestrap, A.P. (1975) The mitochondrial pyruvate carrier. Kinetics and specificity for substrates and inhibitors. *Biochem J* 148: 85-96.
- Halestrap, A.P. (1978) Pyruvate and ketone-body transport across the mitochondrial membrane. Exchange properties, pH-dependence and mechanism of the carrier. *Biochem J* 172: 377-387.
- Herzig, S., Raemy, E., Montessuit, S., Veuthey, J.L., Zamboni, N., Westermann, B., et al. (2012) Identification and functional expression of the mitochondrial pyruvate carrier. *Science* 337: 93-96.
- Hirumi, H., and Hirumi, K. (1989) Continuous cultivation of *Trypanosoma brucei* blood stream forms in a medium containing a low concentration of serum protein without feeder cell layers. *J Parasitol* 75: 985-989.
- Hofmann, K., and Stoffel, W. (1993) TMbase - a database of membrane spanning proteins segments. *Biol Chem Hoppe-Seyler* 374: 166.
- Huelsenbeck, J.P., and Ronquist, F. (2001) MRBAYES: Bayesian inference of phylogenetic trees. *Bioinformatics* 17: 754-755.
- King, N. (2007) Amino acids and mitochondria. In *Mitochondria: The Dynamic Organelle*. Schaffer, S.W., and Suleiman, M.S. (eds). New York: Springer Verlag, pp. 151-166.
- Krogh, A., Larsson, B., von, H.G., and Sonnhammer, E.L. (2001) Predicting transmembrane protein topology with a hidden Markov model: application to complete genomes. *J Mol Biol* 305: 567-580.
- Lamour, N., Riviere, L., Coustou, V., Coombs, G.H., Barrett, M.P., and Bringaud, F. (2005) Proline metabolism in procyclic *Trypanosoma brucei* is down-regulated in the presence of glucose. *J Biol Chem* 280: 11902-11910.
- Lee, Y., Nishizawa, T., Yamashita, K., Ishitani, R., and Nureki, O. (2015) Structural basis for the facilitative diffusion mechanism by SemiSWEET transporter. *Nat Commun* 6: 6112.
- Li, C.L., Wang, M., Ma, X.Y., and Zhang, W. (2014) NRGA1, a putative mitochondrial pyruvate carrier, mediates ABA regulation of guard cell ion channels and drought stress responses in *Arabidopsis*. *Mol Plant* 7: 1508-1521.
- Linstead, D.J., Klein, R.A., and Cross, G.A. (1977) Threonine catabolism in *Trypanosoma brucei*. *J Gen Microbiol* 101: 243-251.
- de Macedo, J.P., Schumann, B.G., Niemann, M., Barrett, M.P., Vial, H., Maser, P., et al. (2015) An atypical mitochondrial carrier that mediates drug action in *Trypanosoma brucei*. *PLoS Pathog* 11: e1004875.
- Mach, J., Poliak, P., Matuskova, A., Zarsky, V., Janata, J., Lukes, J., and Tachezy, J. (2013) An advanced system of the mitochondrial processing peptidase and core protein family in *Trypanosoma brucei* and multiple origins of the Core I subunit in eukaryotes. *Genome Biol Evol* 5: 860-875.
- Mazet, M., Morand, P., Biran, M., Bouyssou, G., Courtois, P., Daulouede, S., et al. (2013) Revisiting the central metabolism of the bloodstream forms of *Trypanosoma*

# AQ1

## Mitochondrial pyruvate carrier in *Trypanosoma brucei* 15

- 1070 *brucei*: production of acetate in the mitochondrion is  
1071 essential for parasite viability. *PLoS Negl Trop Dis* 7:  
1072 e2587.
- 1073 Medina-Acosta, E., and Cross, G.A. (1993) Rapid isolation of  
1074 DNA from trypanosomatid protozoa using a simple 'mini-  
1075 prep' procedure. *Mol Biochem Parasitol* 59: 327-329.
- 1076 Millerioux, Y., Morand, P., Biran, M., Mazet, M., Moreau, P.,  
1077 Wargnies, M., *et al.* (2012) ATP synthesis-coupled and -  
1078 uncoupled acetate production from acetyl-CoA by  
1079 mitochondrial acetate:succinate CoA-transferase and  
1080 acetyl-CoA thioesterase in *Trypanosoma*. *J Biol Chem*  
1081 287: 17186-17197.
- 1082 Millerioux, Y., Ebikeme, C., Biran, M., Morand, P.,  
1083 Bouyssou, G., Vincent, I.M., *et al.* (2013) The threonine  
1084 degradation pathway of the *Trypanosoma brucei* procyclic  
1085 form: the main carbon source for lipid biosynthesis is  
1086 under metabolic control. *Mol Microbiol* 90: 114-129.
- 1087 Nakai, K., and Horton, P. (1999) PSORT: a program for  
1088 detecting sorting signals in proteins and predicting their  
1089 subcellular localization. *Trends Biochem Sci* 24: 34-36.
- 1090 Nalecz, M.J., Nalecz, K.A., and Azzi, A. (1991) Purification and  
1091 functional characterisation of the pyruvate (monocarboxylate)  
1092 carrier from baker's yeast mitochondria (*Saccharomyces cer-  
1093 visiae*). *Biochim Biophys Acta* 1079: 87-95.
- 1094 Panigrahi, A.K., Ogata, Y., Zikova, A., Anupama, A., Dalley,  
1095 R.A., Acestor, N., *et al.* (2009) A comprehensive analysis  
1096 of *Trypanosoma brucei* mitochondrial proteome. *Proteo-  
1097 mics* 9: 434-450.
- 1098 Papa, S., Francavilla, A., Paradies, G., and Meduri, B.  
1099 (1971) The transport of pyruvate in rat liver mitochondria.  
1100 *FEBS Lett* 12: 285-288.
- 1101 Quijada, L., Guerra-Giraldez, C., Drozd, M., Hartmann, C.,  
1102 Irmer, H., Ben-Dov, C., *et al.* (2002) Expression of the  
1103 human RNA-binding protein HuR in *Trypanosoma brucei*  
1104 increases the abundance of mRNAs containing AU-rich  
1105 regulatory elements. *Nucleic Acids Res* 30: 4414-4424.
- 1106 Roldan, A., Comini, M.A., Crispo, M., and Krauth-Siegel,  
1107 R.L. (2011) Lipoamide dehydrogenase is essential for  
1108 both bloodstream and procyclic *Trypanosoma brucei*. *Mol  
1109 Microbiol* 81: 623-639.
- 1110 Ruepp, S., Furger, A., Kurath, U., Renggli, C.K., Hemphill, A.,  
1111 Brun, R., and Roditi, I. (1997) Survival of *Trypanosoma  
1112 brucei* in the tsetse fly is enhanced by the expression of  
1113 specific forms of procyclin. *J Cell Biol* 137: 1369-1379.
- 1114 Sanchez, M.A. (2013) Molecular identification and charac-  
1115 terization of an essential pyruvate transporter from *Trypa-  
1116 nosoma brucei*. *J Biol Chem* 288: 14428-14437.
- 1117 Smid, O., Horakova, E., Vilimova, V., Hrdy, I., Cammack,  
1118 R., Horvath, A., *et al.* (2006) Knock-downs of iron-sulfur  
1119 cluster assembly proteins IscS and IscU down-regulate  
the active mitochondrion of procyclic *Trypanosoma bru-*1120  
*cei*. *J Biol Chem* 281: 28679-28686. 1121
- Southern, E. (2006) Southern blotting. *Nat Protoc* 1:1122  
518-525. 1123
- Spitznagel, D., Ebikeme, C., Biran, M., Nic a', B.N.,1124  
Bringaud, F., Hennehan, G.T., and Nolan, D.P. (2009) Ala-1125  
nine aminotransferase of *Trypanosoma brucei* - a key1126  
role in proline metabolism in procyclic life forms. *FEBS J*1127  
276: 7187-7199. 1128
- Subrtova, K., Panicucci, B., and Zikova, A. (2015)1129  
ATPaseTb2, a unique membrane-bound FoF1-1130  
ATPase component, is essential in bloodstream and1131  
dyskinetoplastic trypanosomes. *PLoS Pathog* 11:1132  
e1004660. 1133
- Sykes, S.E., and Hajduk, S.L. (2013) Dual functions of1134  
alpha-ketoglutarate dehydrogenase E2 in the Krebs cycle1135  
and mitochondrial DNA inheritance in *Trypanosoma bru-*1136  
*cei*. *Eukaryot Cell* 12: 78-90. 1137
- Timon-Gomez, A., Proft, M., and Pascual-Ahuir, A. (2013)1138  
Differential regulation of mitochondrial pyruvate carrier1139  
genes modulates respiratory capacity and stress toler-1140  
ance in yeast. *PLoS One* 8: e79405. 1141
- Urbaniak, M.D., Guther, M.L., and Ferguson, M.A. (2012)1142  
Comparative SILAC proteomic analysis of *Trypanosoma*1143  
*brucei* bloodstream and procyclic lifecycle stages. *PLoS*1144  
*One* 7: e36619. 1145
- Vanderperre, B., Bender, T., Kunji, E.R., and Martinou,1146  
J.C. (2014) Mitochondrial pyruvate import and its1147  
effects on homeostasis. *Curr Opin Cell Biol* 33C:1148  
41. 1149
- Vondruskova, E., van den Burg, J., Zikova, A., Ernst,1150  
N.L., Stuart, K., Benne, R., and Lukes, J. (2005) RNA1151  
interference analyses suggest a transcript-specific regu-1152  
latory role for mitochondrial RNA-binding proteins1153  
MRP1 and MRP2 in RNA editing and other RNA proc-1154  
essing in *Trypanosoma brucei*. *J Biol Chem* 280:1155  
2429-2438. 1156
- Wirtz, E., Leal, S., Ochatt, C., and Cross, G.A. (1999) A1157  
tightly regulated inducible expression system for condi-1158  
tional gene knock-outs and dominant-negative genetics1159  
in *Trypanosoma brucei*. *Mol Biochem Parasitol* 99:1160  
89-101. 1161

## Supporting information 1162

Additional supporting information may be found in the1163  
online version of this article at the publisher's web-site. 1164

1165